

<sup>15</sup>Varian Associates, Palo Alto, Calif.; A. L. Bloom, Appl. Opt. **1**, 61 (1962).

<sup>16</sup>E. S. Ensberg, Phys. Rev. **153**, 36 (1967); Phys. Rev. **164**, 270 (1967).

<sup>17</sup>H. G. Robinson, E. S. Ensberg, and H. G. Dehmelt, Bull. Am. Phys. Soc. **3**, 9 (1968).

<sup>18</sup>F. D. Bedard (private communication).

<sup>19</sup>R. J. Blume, Rev. Sci. Instrum. **32**, 743 (1961).

<sup>20</sup>C. C. Bouchiat, M. A. Bouchiat, and L. C. L. Pottier, Phys. Rev. **181**, 144 (1969); P. L. Bender and V. W. Cohen, *Sixth International Conference on the Physics of Electrons and Atomic Collisions: Abstract* (MIT Press, Cambridge, Mass., 1969); F. Hartmann and F. Hartmann-Bourton, Phys. Rev. A **2**, 1885

(1970).

<sup>21</sup>J. J. Wright, Phys. Rev. A **6**, 524 (1972).

<sup>22</sup>T. Crane, D. Casperson, P. Crane, P. Egan, V. W. Hughes, R. Stambaugh, P. A. Thompson, and G. zu Putlitz, Phys. Rev. Lett. **27**, 474 (1971); D. Farart, P. M. McIntyre, D. Y. Stowell, V. L. Telegdi, R. DeVoe, and R. A. Swanson, Phys. Rev. Lett. **27**, 1336 (1971); see, e.g., P. A. Thompson, J. J. Amato, P. Crane, V. W. Hughes, R. M. Mobley, G. zu Putlitz, and J. L. Rothberg [Phys. Rev. Lett. **22**, 163 (1968)] for earlier treatment of the pressure shift.

<sup>23</sup>J. J. Wright, L. C. Balling, and R. H. Lambert, Phys. Rev. A **1**, 1018 (1970).

## Polarization Correlations in Atomic-Field Bremsstrahlung\*

H. K. Tseng and R. H. Pratt

*Department of Physics, University of Pittsburgh, Pittsburgh, Pennsylvania 15260*

(Received 4 December 1972)

Atomic bremsstrahlung-polarization correlations between incident electron and emitted photon are discussed for incident-electron kinetic energies in the range from 5 keV to 1 MeV. Results are reported from an exact numerical calculation in partial-wave formulation using screened potentials. It is shown that bremsstrahlung can be used as an analyzer of polarized electrons, a transmitter of polarization from electrons to photons, or a source of polarized radiation. Comparisons are made with previous work where available.

### I. INTRODUCTION

Recently it has become possible to predict rather accurately atomic-field bremsstrahlung cross sections for incident-electron kinetic energies  $T_1 (\equiv E_1 - m_e c^2)$  in the range 5 keV to 1 MeV. These predictions are obtained numerically for screened central potentials, using an exact partial-wave formulation. We<sup>1</sup> have reported results obtained in this way for the unpolarized case. Good agreement was obtained with recent experiments.<sup>2</sup>

We wish to report here results obtained in the same calculations for the bremsstrahlung-polarization correlations. In this work it is assumed that the final electron is not observed, and consequently we only consider correlations involving incident electron and final photon. Interest in this subject was increased when it was discovered that electrons from  $\beta$  decay and  $\mu$ - $e$  decay<sup>3</sup> are polarized. In recent years considerable effort has gone into the development of high-intensity collimated polarized-electron beams. However, in the energy region considered here the only polarization property of bremsstrahlung which has been studied experimentally is linear polarization.<sup>4-6</sup> Predictions for the polarization correlations in the Born approximation were given by Gluckstern, Hull, and Breit; Gluckstern and Hull; Banerjee; McVoy; and Fronsdal and Überall.<sup>7</sup> The corresponding result

averaged over initial and summed over final polarizations is the well-known Bethe-Heitler formula.<sup>8</sup> Theoretical predictions beyond the Born approximation were given for the nonrelativistic region by Kirkpatrick and Wiedmann,<sup>9</sup> and for the extreme high-energy region by Olsen and Maximon.<sup>10</sup> In the energy region we consider here the only results available are (i) one value for the asymmetry function obtained by Rozics and Johnson<sup>11</sup> using exact electron point-Coulomb wave functions in a partial-wave expansion, (ii) a few results for linear polarization reported by Brysk, Zerby, and Penny<sup>12</sup> from a numerical calculation similar to ours, and (iii) calculations by Haug<sup>13</sup> for the special situation in which all the incident electron energy is radiated (the tip region). Haug used approximate electron wave functions to obtain analytic results valid (neglecting screening) at least for low- $Z$  elements. The purpose of this paper is to survey the types of polarization correlations which exist, to examine the dependence of the correlations on energy and  $Z$ , and to see how well they are predicted by simpler calculations. A more detailed tabulation is not now feasible, owing to the length of the computer calculations.

In Sec. II we describe the mathematical formalism for these calculations and our numerical methods. In Sec. III we discuss the behavior of the polarization correlations at small and large photon

angles, at extreme low and high energies, and for low atomic number  $Z$ . Then we present our numerical results and we comment on the validity of Born approximation and the importance of atomic-electron screening effects. Comparisons are made with previous theory and experiment when available.

## II. THEORY

We use the formalism of our atomic bremsstrahlung work<sup>1,14</sup> and write the bremsstrahlung cross section, differential in photon energy and angle, and in final electron angle, as

$$d\sigma = (2\pi)^{-5} (E_1 E_2 p_2 k^2 / p_1) dk d\Omega_k d\Omega_2 |M_{fi}|^2, \quad (2.1)$$

subject to energy conservation

$$E_1 = k + E_2. \quad (2.2)$$

Here we denote the energy and momentum of the initial and final electron as  $(E_1, \vec{p}_1)$  and  $(E_2, \vec{p}_2)$ , and the energy and momentum of the photon as  $(k, \vec{k})$ . The atomic bremsstrahlung matrix element

$$M_{fi} = (2\pi\alpha/k)^{1/2} \int d^3r \psi_2^\dagger \vec{\alpha} \cdot \vec{\epsilon}^* \psi_1 e^{-i\vec{k}\cdot\vec{r}}, \quad (2.3)$$

where  $\vec{\epsilon}$  is a complex unit vector describing photon polarization such that  $\vec{\epsilon} \cdot \vec{\epsilon}^* = 1$  and  $\vec{\epsilon} \cdot \vec{k} = 0$ , and in the spinor representation

$$\vec{\alpha} = \begin{pmatrix} 0 & \vec{\sigma} \\ \vec{\sigma} & 0 \end{pmatrix},$$

with  $\vec{\sigma}$  the familiar  $2 \times 2$  Pauli matrices.  $\psi_1$  and  $\psi_2$  are the initial and final electron wave functions asymptotically normalized to unit-amplitude plane waves of four-momentum  $(E_1, \vec{p}_1)$  and  $(E_2, \vec{p}_2)$  plus outgoing or incoming spherical waves, respectively. We chose a coordinate system centered at the atomic nucleus with the  $z$  axis  $\hat{z}$  along  $\vec{k}$ ,  $\hat{y}$  along  $\vec{k} \times \vec{p}_1$ , and  $\hat{x}$  in the  $(\vec{k}, \vec{p}_1)$  plane (the emission plane). This choice leads to substitution rules for the matrix element  $M_{fi}$  which simplify our discussion of the polarization correlations.

Now let us consider the photon polarization.<sup>15</sup> The wave function of a photon with a definite momentum  $\vec{k}$  and a definite polarization is

$$A^0 = 0$$

and

$$\vec{A}(x) = (2\pi/k)^{1/2} e^{-ikx} \vec{\epsilon}.$$

We describe the photon polarization with Stokes parameters

$$\xi_\mu = \epsilon_s^\dagger \sigma_\mu \epsilon_s \quad (\mu = 0, 1, 2, 3), \quad (2.4)$$

where

$$\epsilon_s = \begin{pmatrix} \epsilon_1 \\ \epsilon_2 \end{pmatrix}, \quad \sigma_0 = 1,$$

and

$$\vec{\epsilon} = \epsilon_1 \hat{x} + \epsilon_2 \hat{y}, \quad \text{with } |\epsilon_1|^2 + |\epsilon_2|^2 = 1.$$

In order to specify the polarization completely, the three parameters  $\vec{\xi}$  must be determined, e.g., by polarization measurements with respect to three linearly independent bases. For these bases, we could take (i) two states of linear polarization with perpendicular planes of polarizations, (ii) two other states of linear polarization making angles  $\pi/4$  with the planes of polarization in (i), and (iii) the two states of left and right circularly polarized light.

We use the spinor representation for Dirac electron wave functions. In this representation any matrix element between four-component states may be reduced to matrix elements between two-component spinors

$$\chi = \sum_s a_s \chi^s,$$

with

$$\chi^\dagger \chi = 1, \quad \chi^{1/2} = \begin{pmatrix} 1 \\ 0 \end{pmatrix}, \quad \chi^{-1/2} = \begin{pmatrix} 0 \\ 1 \end{pmatrix}.$$

The two-component spinor  $\chi$  is the large component of the asymptotic constant four-component spinor corresponding to an asymptotic free-particle plane-wave state. The small component of the asymptotic spinor may be written as  $(\vec{\sigma} \cdot \vec{p})/(E+1)\chi$ . This gives a simple way to separate out quantities depending on polarization. The polarization state of an electron is specified by its spin direction  $\vec{\xi}$  in the rest system, with

$$\begin{aligned} \xi_1 &= \vec{\xi} \cdot (\vec{y} \times \vec{p}) / |\vec{y} \times \vec{p}|, \\ \xi_2 &= \vec{\xi} \cdot \hat{y}, \quad \xi_3 = \vec{\xi} \cdot \hat{p}; \end{aligned} \quad (2.5)$$

$(\xi_1, \xi_2, \xi_3)$  form a right-handed set.

The spin direction  $\vec{\xi}$  is determined from  $\chi$  by requiring that  $\chi$  be an eigenstate of  $\vec{\sigma} \cdot \vec{\xi}$ :

$$\vec{\sigma} \cdot \vec{\xi} \chi = \chi. \quad (2.6)$$

From Eq. (2.6) we have

$$(1 - \vec{\sigma} \cdot \vec{\xi}) \chi \chi^\dagger = 0.$$

For normalized  $\chi$ , the solution is clearly

$$\chi \chi^\dagger = \frac{1}{2} (1 + \vec{\sigma} \cdot \vec{\xi}), \quad (2.7)$$

permitting the determination of  $\vec{\xi}$  from  $\chi$ . Alternatively, from Eq. (2.6) we have also  $\chi^\dagger \vec{\sigma} \cdot \vec{\xi} \chi = 1$ . In the rest system  $\vec{\xi}$  is the only vector available, so

$$\chi^\dagger \vec{\sigma} \chi = \vec{\xi}. \quad (2.8)$$

The four-component wave functions  $\psi_1$  and  $\psi_2$  are<sup>16</sup> linear in  $\chi_1$  and  $\chi_2$ , respectively. Hence we may write the matrix element  $M_{fi}$  as

$$\begin{aligned} M_{fi} &= (2\pi\alpha/k)^{1/2} \int d^3r \psi_2^\dagger \vec{\alpha} \cdot \vec{\epsilon}^* \psi_1 e^{-i\vec{k}\cdot\vec{r}} \\ &= (2\pi\alpha/k)^{1/2} \chi_2^\dagger M(\vec{\epsilon}) \chi_1. \end{aligned} \quad (2.9)$$

The  $2 \times 2$  matrix  $M(\vec{\epsilon})$  is linear in  $\vec{\epsilon}$  and is some lin-

ear combination of the unit matrix and the Pauli spin matrices  $\vec{\sigma}$ , i. e.,

$$M(\vec{\epsilon}) = \epsilon_1 M_1 + \epsilon_2 M_2,$$

with  $M_1$  and  $M_2$  linear combinations of the unit matrix and the Pauli spin matrices  $\vec{\sigma}$ . Under<sup>16a</sup> the time-reversal transformation  $\mathcal{T}$  the bremsstrahlung matrix element  $M_{fi}$  of Eq. (2.3) becomes

$$\begin{aligned} \mathcal{T} M_{fi} \mathcal{T}^{-1} &= (2\pi\alpha/k)^{1/2} \int d^3r (T\psi_2^*)^\dagger T\vec{\alpha}^* \cdot \vec{\epsilon} T^{-1} T\psi_1^* e^{i\vec{k}\cdot\vec{r}} \\ &= M_{fi}^{\prime*} = M_{fi}^* , \end{aligned}$$

since  $T = i\gamma^1\gamma^3 = T^\dagger = T^{-1} = -T^*$ , where the prime refers to the substitutions

$$\psi(\vec{r}) \rightarrow \begin{pmatrix} \sigma_y & 0 \\ 0 & \sigma_y \end{pmatrix} \psi(\vec{r}), \quad (\epsilon_1, \epsilon_2) \rightarrow (-\epsilon_1, \epsilon_2). \quad (2.10a)$$

As the potential  $V$  is invariant under the time-reversal transformation, the transformed states  $T\psi_1^*$  and  $T\psi_2^*$  are physical states— $T\psi^*$  corresponds to the continuum state asymptotically with opposite space momentum  $\vec{p}$  and opposite spin. This implies the equivalence of two matrix elements, in which the polarization properties are related as

$$\chi \rightarrow \sigma_y \chi, \quad (\epsilon_1, \epsilon_2) \rightarrow (-\epsilon_1, \epsilon_2). \quad (2.10b)$$

In terms of  $\vec{\xi}$  and  $\vec{\zeta}$  these become

$$\begin{aligned} (\zeta_1, \zeta_2, \zeta_3) &\rightarrow (-\zeta_1, \zeta_2, -\zeta_3), \\ (\xi_1, \xi_2, \xi_3) &\rightarrow (-\xi_1, -\xi_2, \xi_3). \end{aligned} \quad (2.11)$$

Thus, we have

$$\chi_2^\dagger (\epsilon_1 M_1 + \epsilon_2 M_2) \chi_1 = (\sigma_y \chi_2)^\dagger (-\epsilon_1 M_1 + \epsilon_2 M_2) \sigma_y \chi_1$$

or

$$\begin{aligned} M_2 &= A(\theta) + iB(\theta)\vec{\sigma}\cdot\hat{y}, \\ M_1 &= iC(\theta)\vec{\sigma}\cdot(\vec{y}\times\vec{p}_1)/|\vec{y}\times\vec{p}_1| + iD(\theta)\vec{\sigma}\cdot\hat{p}_1, \end{aligned} \quad (2.12)$$

where  $\theta$  is the angle between  $\vec{k}$  and  $\vec{p}_1$ ;  $A, B, C$  and  $D$  are complex-valued scalar functions. Here we are assuming that the final electron is not observed, otherwise the four scalar functions would depend on further angular variables.

Integrating the bremsstrahlung differential cross section, Eq. (2.1), over  $d\Omega_2$ , using Eqs. (2.9) and (2.12), and summing over final electron spins, we may write the bremsstrahlung cross section,

$$\sigma(k, \theta, \vec{\xi}_1, \vec{\xi}) = \sigma_0(k, \theta) \left( \frac{1}{2} \sum_{\mu, \nu=0}^3 \xi_{1\mu} \xi_\nu C_{\mu\nu}(k, \theta) \right), \quad (2.13)$$

with  $C_{00} = 1$ ,  $\xi_{10} = 1$ ,  $\xi_0 = 1$ , and

$$\sigma \equiv \frac{k}{Z^2} \frac{d\sigma}{dk d\Omega_k}. \quad (2.14)$$

(Note that  $\xi_{1\mu}$  and  $\xi_\nu$  are not four-vectors.) Here  $\sigma_0(k, \theta)$  is the differential cross section averaged over the initial electron spins and summed over the final photon and electron polarizations:

$$\sigma_0(k, \theta) = \lambda_0 D_{00}(k, \theta), \quad (2.15)$$

with

$$\lambda_0 = 32\alpha E_1 E_2 p_2 k^2 / Z^2 p_1 \quad (2.16)$$

and

$$D_{00}(k, \theta) = \frac{|A|^2 + |B|^2 + |C|^2 + |D|^2}{2(4\pi)^3}. \quad (2.17)$$

The real numbers  $C_{\mu\nu}(k, \theta)$ , satisfying  $|C_{\mu\nu}| < 1$  since cross sections cannot be negative, are the polarization correlations between incident electron and emitted photon. The nonvanishing polarization correlations<sup>17</sup> are

$$\begin{aligned} C_{00} &\equiv 1, \quad C_{03} = -\frac{|A|^2 + |B|^2 - |C|^2 - |D|^2}{2(4\pi)^3 D_{00}}, \\ C_{12} &= \frac{\text{Re}(AC^* + BD^*)}{(4\pi)^3 D_{00}}, \\ C_{32} &= \frac{\text{Re}(AD^* - BC^*)}{(4\pi)^3 D_{00}}, \\ C_{11} &= \frac{\text{Im}(AC^* + BD^*)}{(4\pi)^3 D_{00}}, \\ C_{31} &= \frac{\text{Im}(AD^* - BC^*)}{(4\pi)^3 D_{00}}, \\ C_{20} &= \frac{\text{Im}(AB^* - CD^*)}{(4\pi)^3 D_{00}}, \\ C_{23} &= -\frac{\text{Im}(AB^* + CD^*)}{(4\pi)^3 D_{00}}. \end{aligned} \quad (2.18)$$

Although Eqs. (2.15)–(2.18) were obtained assuming a complete polarization of the photon, i. e.,  $|\vec{\xi}| = 1$ , it is easy to see that they are also valid for a partial polarization,  $|\vec{\xi}| < 1$ , since any statistical mixture can be obtained by incoherent superposition of two appropriately chosen pure states. That the only nonzero polarization correlations are as just given follows from the application of Eq. (2.11) to Eq. (2.13).

In partial-wave expansion<sup>1,14</sup> the atomic bremsstrahlung-polarization correlations are given by

$$\begin{aligned} C_{00} &\equiv 1, \\ C_{03} &= D_{00}^{-1} \sum_{k_2 k_1 \bar{k}_1} (-)^{l_1 + l_1} \cos \delta \sum_{m_1 m_2} \{ A_+^* \bar{A}_+^- \\ &\quad + A_+^* \bar{A}_-^- + A_+^- \bar{A}_+^+ + A_-^- \bar{A}_+^+ \}, \\ C_{12} &= D_{00}^{-1} \sum_{k_2 k_1 \bar{k}_1} (-)^{l_1 + l_1} \cos \delta \sum_{m_1 m_2} \{ A_{21} \cos \theta \\ &\quad + A_{22} \sin \theta \}, \\ C_{32} &= D_{00}^{-1} \sum_{k_2 k_1 \bar{k}_1} (-)^{l_1 + l_1} \cos \delta \sum_{m_1 m_2} \{ A_{21} \sin \theta \} \end{aligned}$$

$$\begin{aligned}
& -A_{22} \cos \theta\}, \\
C_{11} = D_{00}^{-1} \sum_{\kappa_2 \kappa_1 \bar{\kappa}_1} (-)^{\bar{l}_1 + l_1} \sin \delta \sum_{m=1, m_2} \{ & A_{11} \cos \theta \\
& + A_{12} \sin \theta\}, \\
C_{31} = D_{00}^{-1} \sum_{\kappa_2 \kappa_1 \bar{\kappa}_1} (-)^{\bar{l}_1 + l_1} \sin \delta \sum_{m=1, m_2} \{ & A_{11} \sin \theta \\
& - A_{12} \cos \theta\}, \\
C_{20} = D_{00}^{-1} \sum_{\kappa_2 \kappa_1 \bar{\kappa}_1} (-)^{\bar{l}_1 + l_1} \sin \delta \sum_{m=1, m_2} \{ & A_{11}^+ \bar{A}_{11}^- \\
& + A_{12}^+ \bar{A}_{12}^- - A_{12}^- \bar{A}_{12}^+ - A_{11}^- \bar{A}_{11}^+\}, \\
C_{23} = D_{00}^{-1} \sum_{\kappa_2 \kappa_1 \bar{\kappa}_1} (-)^{\bar{l}_1 + l_1} \sin \delta \sum_{m=1, m_2} \{ & A_{11}^- \bar{A}_{11}^+ \\
& + A_{12}^+ \bar{A}_{12}^- - A_{12}^- \bar{A}_{12}^+ - A_{11}^+ \bar{A}_{11}^-\}.
\end{aligned} \quad (2.19)$$

Here

$$D_{00} = \sum_{\kappa_2 \kappa_1 \bar{\kappa}_1} (-)^{\bar{l}_1 + l_1} \cos \delta \sum_{m=1, m_2} \{ A_{11}^+ \bar{A}_{11}^+ + A_{12}^+ \bar{A}_{12}^+ + A_{12}^- \bar{A}_{12}^- + A_{11}^- \bar{A}_{11}^- \}; \quad (2.20)$$

$$\begin{aligned}
\delta & \equiv \delta_{\kappa_1} - \delta_{\bar{\kappa}_1}; \\
A_{21} & = A_{12}^+ \bar{A}_{12}^- + A_{12}^- \bar{A}_{12}^+ - A_{11}^+ \bar{A}_{11}^- - A_{11}^- \bar{A}_{11}^+, \\
A_{22} & = A_{11}^- \bar{A}_{11}^+ + A_{12}^+ \bar{A}_{12}^- - A_{12}^- \bar{A}_{12}^+ - A_{11}^+ \bar{A}_{11}^-, \\
A_{11} & = A_{11}^+ \bar{A}_{11}^- + A_{12}^+ \bar{A}_{12}^- - A_{12}^- \bar{A}_{12}^+ - A_{11}^- \bar{A}_{11}^+, \\
A_{12} & = A_{12}^+ \bar{A}_{12}^- + A_{12}^- \bar{A}_{12}^+ - A_{11}^- \bar{A}_{11}^+ - A_{11}^+ \bar{A}_{11}^-; \\
A_{\frac{1}{2}}^+(m) & = C_{\kappa_1, m-1}^+ Y_{l_1, m-1+1/2}(\hat{p}_1) R_{\kappa_2 \kappa_1}^+(m), \\
A_{\frac{1}{2}}^-(m) & = C_{\kappa_1, m+1}^+ Y_{l_1, m+1+1/2}(\hat{p}_1) R_{\kappa_2 \kappa_1}^-(m).
\end{aligned} \quad (2.21)$$

The reduced partial-wave matrix element  $\bar{A}_{\frac{1}{2}}^{\pm}$  is obtained from  $A_{\frac{1}{2}}^{\pm}$  in Eqs. (2.22) by replacing  $\kappa_1$  with  $\bar{\kappa}_1$ . The symbol  $\kappa$  is a compact notation for the total angular momentum  $j$  and parity, with  $\kappa = \mp(j + \frac{1}{2})$  as  $j = l \pm \frac{1}{2}$  (or  $j = l' \mp \frac{1}{2}$ ); the symbol  $C_{\kappa, m}^{\pm} \equiv C(l_{\frac{1}{2}}^{\pm}; m - s, s = \pm \frac{1}{2})$  are the Clebsch-Gordan coefficients. In Eqs. (2.22) the  $R$  matrix element is defined as

$$R_{\kappa_2 \kappa_1}^{\pm}(m) = \sum_{n=1}^2 Q_n^{\pm}(m) \sum_l P_n^{\pm}(m) s_n, \quad (2.23)$$

where the index  $l$  runs from  $|l_2' - l_1|$  to  $(l_2' + l_1)$  in steps of 2 for  $n=1$ , and from  $|l_2 - l_1'|$  to  $(l_2 + l_1')$  in steps of 2 for  $n=2$ . The  $Q$ 's and  $P$ 's in Eqs. (2.23) are related to the Clebsch-Gordan coefficient and the 3- $j$  symbol by

$$\begin{aligned}
Q_{\frac{1}{2}}^+(m) & = \eta_{\kappa_2} (-)^{m \mp 1/2} [(2l_2' + 1)(2l_1 + 1)]^{1/2} C_{\frac{1}{2}}^+ C_1^{\mp}, \\
Q_{\frac{1}{2}}^-(m) & = -\eta_{\kappa_1} (-)^{m \mp 1/2} [(2l_2 + 1)(2l_1' + 1)]^{1/2} C_{\frac{1}{2}}^+ C_1^{\mp}, \\
P_{\frac{1}{2}}^+(m) & = (-)^{(l_2' + l_1 + 1)/2} T(l_2', l_1, l; m \mp \frac{1}{2}), \\
P_{\frac{1}{2}}^-(m) & = (-)^{(l_2 + l_1' + 1)/2} T(l_2, l_1', l; m \mp \frac{1}{2}),
\end{aligned} \quad (2.24)$$

with

$$T(l_2, l_1, l; m) \equiv (2l + 1) \begin{pmatrix} l_2 & l_1 & l \\ 0 & 0 & 0 \end{pmatrix} \begin{pmatrix} l_2 & l_1 & l \\ -m & m & 0 \end{pmatrix}, \quad (2.25)$$

$$\begin{aligned}
C_n^+ & = \eta_{\kappa_n} [l_n + \eta_{\kappa_n} m_n + \frac{1}{2}] / (2l_n + 1)^{1/2}, \\
C_n^- & = [(l_n - \eta_{\kappa_n} m_n + \frac{1}{2}) / (2l_n + 1)]^{1/2} \\
& \quad (n = 1, 2, 1', 2'),
\end{aligned}$$

$$\begin{aligned}
\eta_{\kappa} & \equiv -\kappa / |\kappa|, \quad \eta_{\kappa_1'} \equiv -\eta_{\kappa_1}, \quad \eta_{\kappa_2'} \equiv -\eta_{\kappa_2}, \\
l_{n'} & = l_n', \quad m_{n'} \equiv m_n.
\end{aligned}$$

The  $s$  integrals in Eqs. (2.23) are given by

$$\begin{aligned}
s_1 & = \int_0^{\infty} dr j_1(kr) g_{\kappa_1} f_{\kappa_2}, \\
s_2 & = \int_0^{\infty} dr j_1(kr) g_{\kappa_2} f_{\kappa_1},
\end{aligned} \quad (2.26)$$

where  $g_{\kappa}$  and  $f_{\kappa}$  satisfy the Dirac radial wave functions,

$$\begin{aligned}
dg/dr & = [E + 1 - V(r)] f - \kappa g/r, \\
df/dr & = -[E - 1 - V(r)] g + \kappa f/r,
\end{aligned} \quad (2.27)$$

in the screened central potential  $V(r)$  for the atom in question. The results presented in this paper were calculated from Eqs. (2.19). The  $s$  integrals, given in Eqs. (2.26), are the basic integrals to be obtained numerically. The numerical method and its accuracy have been discussed in our previous bremsstrahlung work.<sup>1,14</sup>

### III. RESULTS AND DISCUSSION

We first discuss the behavior of the atomic-field bremsstrahlung-polarization correlations in several special situations: for small and large photon angles, at extreme low and high energies, and for low atomic number  $Z$ . Then we present data for each of the correlations.

#### A. Behavior of the Polarization Correlations for Small and Large Photon Angles

We have written in Eqs. (2.19) expressions for the seven polarization correlations in terms of reduced partial-wave matrix elements  $A_{\frac{1}{2}}^{\pm}$  and initial continuum-wave-function phase shifts. Some general information can be deduced from these questions concerning the behavior of the polarization correlations at small and large photon angles. From the definitions of the reduced partial-wave matrix elements  $A_{\frac{1}{2}}^{\pm}$ , Eqs. (2.22), by expanding the spherical harmonics in terms of small  $\theta$  (or  $\pi - \theta$ ) we see that only terms like  $A_{\frac{1}{2}}^+ \bar{A}_{\frac{1}{2}}^+$  or  $A_{\frac{1}{2}}^- \bar{A}_{\frac{1}{2}}^-$  in Eqs. (2.19)–(2.21) do not vanish for forward (and backward) photon angles. Thus the unpolarized angular distribution  $\sigma_0(k, \theta)$  does not vanish for forward (and backward) photon angles, while all the polarization correlations except  $C_{32}$  vanish in the forward and backward directions. For small and large photon angles the polarization correlations  $C_{20}$ ,  $C_{23}$ ,  $C_{11}$ , and  $C_{12}$  go as  $\theta$ , while  $C_{03}$  and  $C_{31}$  go as  $\theta^2$  and  $C_{32}$  is of or-

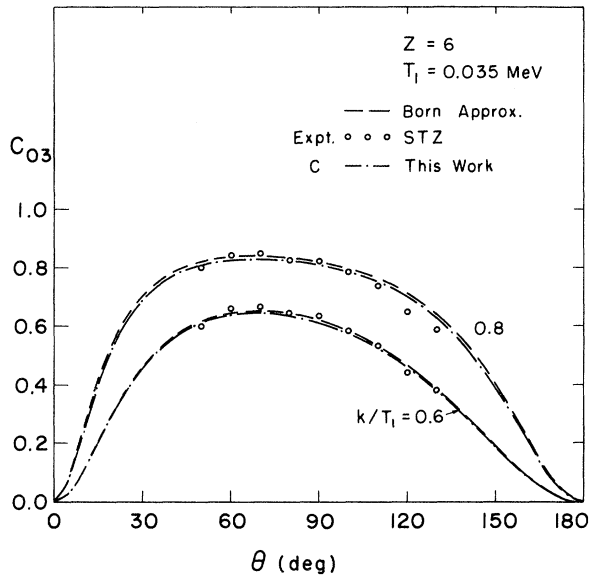


FIG. 1. Atomic bremsstrahlung-polarization correlation  $C_{03}$  for the case  $Z=6$ ,  $T_1=0.035$  MeV. The symbol C refers to the point-Coulomb potential. The numbers attached to the curves give the value of  $k/T_1$  unless otherwise specified.

der 1. Also, for small photon angles one has the identity  $C_{23} = -C_{11}$ , while for large photon angles one has  $C_{23} = C_{11}$ .

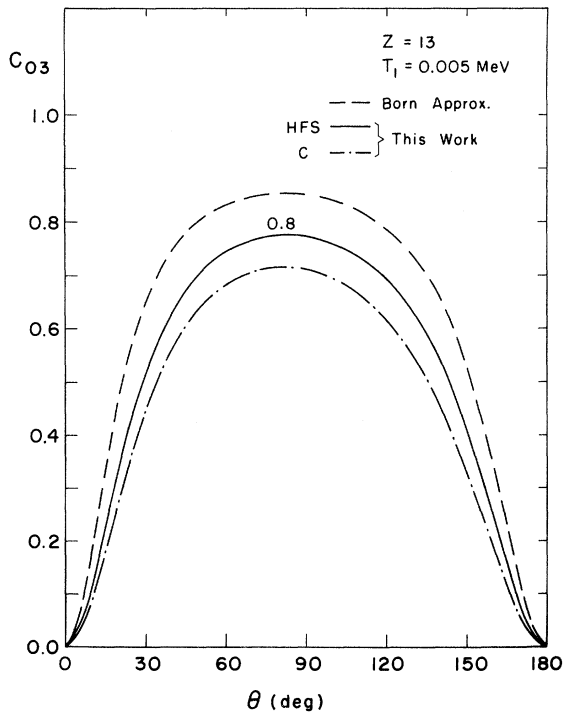


FIG. 2. Same as Fig. 1 except that  $Z=13$ ,  $T_1=0.005$  MeV. The symbol HFS refers to the Hartree-Fock-Slater potential with  $\frac{2}{3}$  of the Slater's exchange.

**B. Behavior of the Polarization Correlations at Extreme Low and High Energies and for Low Atomic Number  $Z$**

In the nonrelativistic theory,  ${}^9\vec{\alpha} \cdot \vec{\epsilon}^*$  in the matrix element  $M_{fi}$  of Eq. (2.3) is replaced by  $\vec{p} \cdot \vec{\epsilon}^*$  and all the dependence on electron spins disappears. This leads to a differential cross section proportional to  $(1 + C_{03} \xi_3)$ , and all the polarization correlations except  $C_{03}$  vanish. At low energies, the polarization correlation  $C_{03}$  is positive which indicates that the radiation is polarized prevalently parallel to the emission plane (the plane through  $\vec{p}_1$  and  $\vec{k}$ ). That is, the electric vector of the radiation is in the plane of emission, which is what would be expected from classical considerations. On the other hand, at high energies<sup>10</sup> the radiation is in general elliptically polarized with the major axis of the polarization ellipse always perpendicular to the plane of emission; i. e., the photons of high energy are emitted in the plane of the magnetic vector. Also, at high energies the linear polarization is independent of the polarization of the initial electron. The independence of the linear polarization on the initial electron spin is also predicted by Born approximation.<sup>7</sup> However, this is not true in general, which has already been pointed out by Haug's calculations.<sup>13</sup> In the extreme high-energy limit<sup>10</sup> as well as in the limit of Born approximation<sup>7</sup> the polarization correlations  $C_{03}$ ,  $C_{12}$ , and  $C_{32}$  are of order 1; i. e., they do not vanish with large  $E$  or small  $Z$ .

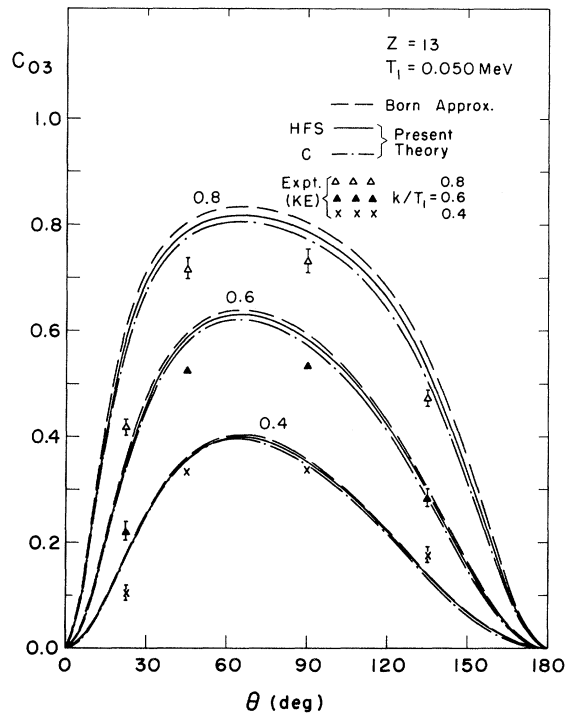


FIG. 3. Same as Fig. 1 except that  $Z=13$ ,  $T_1=0.050$  MeV.

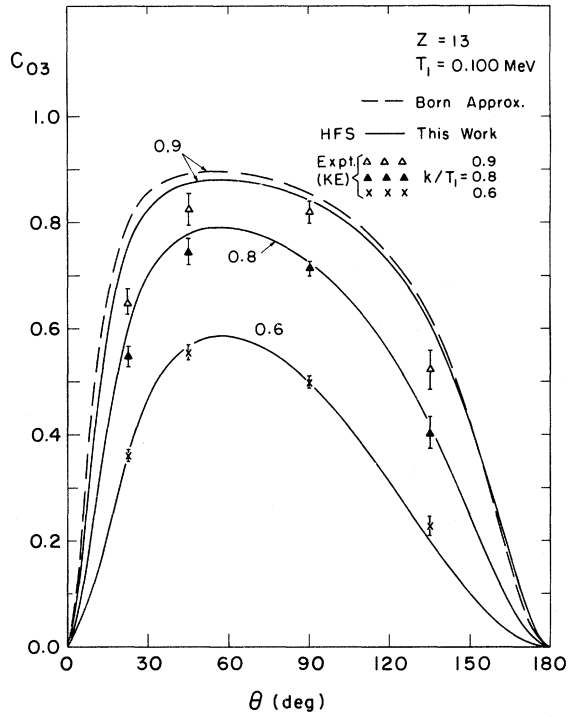


FIG. 4. Same as Fig. 1 except that  $Z=13$ ,  $T_1=0.100$  MeV.

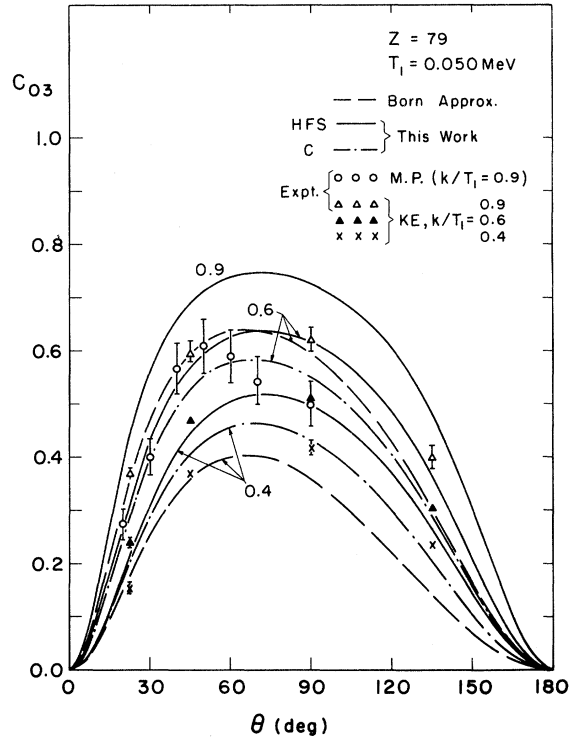


FIG. 6. Same as Fig. 1 except that  $Z=79$ ,  $T_1=0.050$  MeV.

In the small- $Z$  limit, the polarization correlations  $C_{20}$ ,  $C_{23}$ ,  $C_{31}$ , and  $C_{11}$  vanish linearly with  $a \equiv Z\alpha$ ; they also vanish in the large- $E$  limit. (Unlike atomic photoelectric effect no polarization correlations are of order  $a^2$ .)

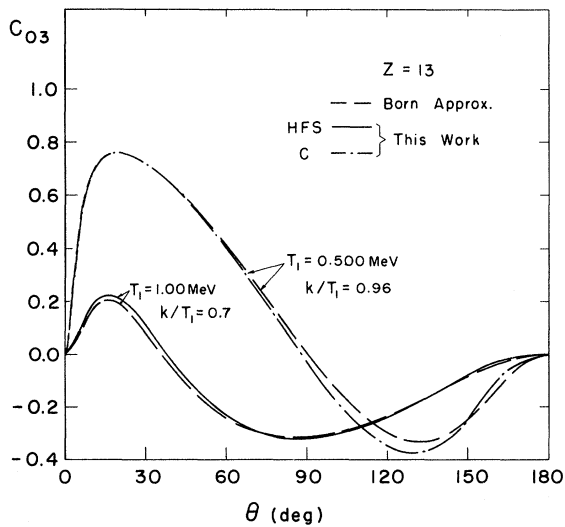


FIG. 5. Same as Fig. 1 except that  $Z=13$ ,  $T_1=0.500$  and  $1.00$  MeV.

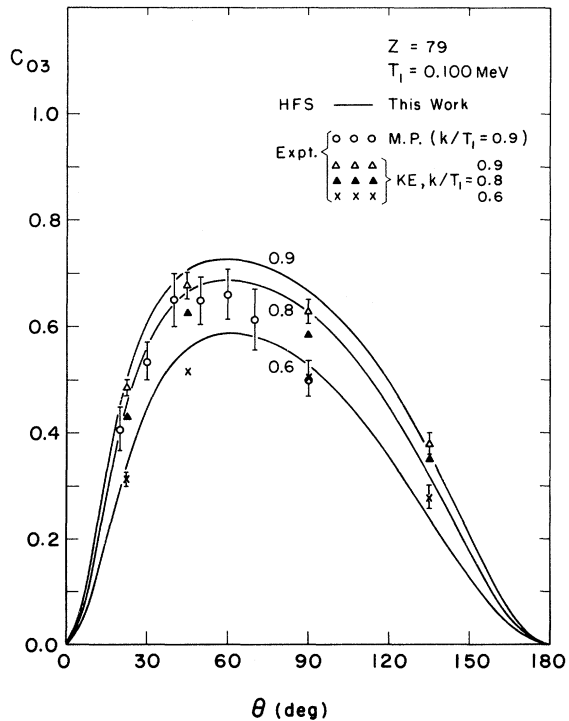


FIG. 7. Same as Fig. 1 except that  $Z=79$ ,  $T_1=0.100$  MeV.

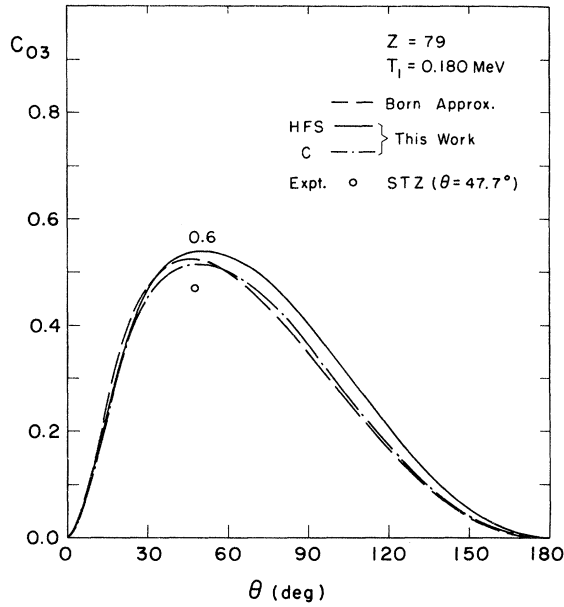


FIG. 8. Same as Fig. 1 except that  $Z=79$ ,  $T_1=0.180$  MeV.

C. Polarization Correlation  $C_{03}$

The polarization correlation  $C_{03}$  reflects the fact that beginning with unpolarized electrons one can produce photons linearly polarized parallel or perpendicular to the emission plane. Increasing positive (or negative) values of this correlation indicate that the radiation is polarized more nearly

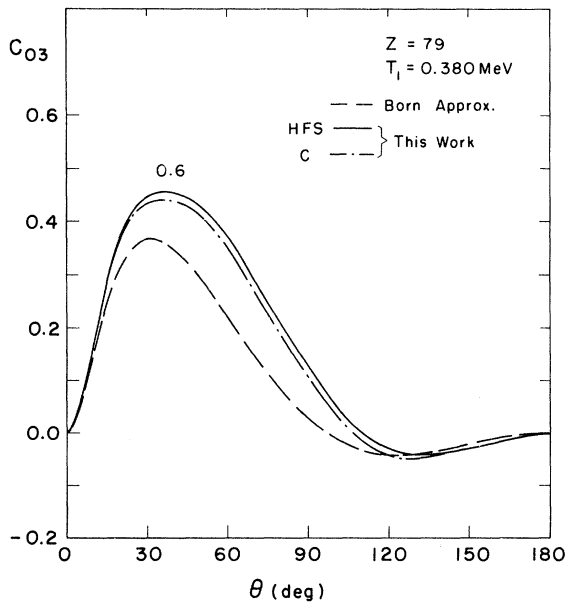


FIG. 9. Same as Fig. 1 except that  $Z=79$ ,  $T_1=0.380$  MeV.

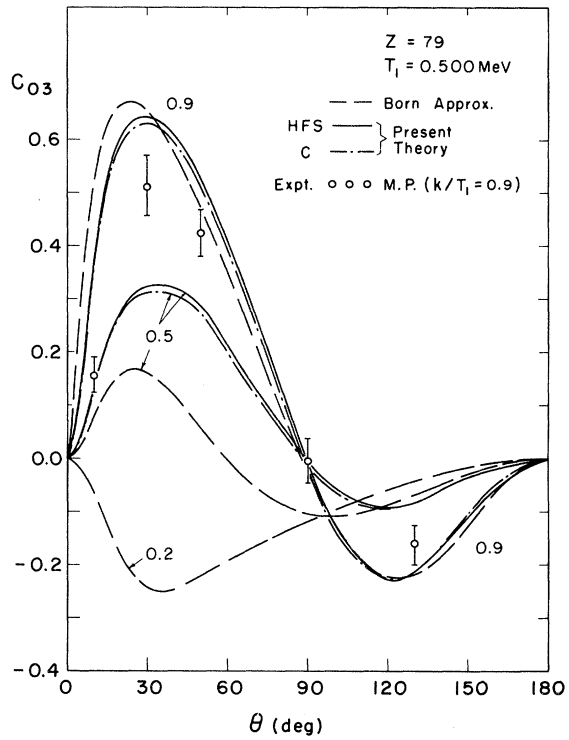


FIG. 10. Same as Fig. 1 except that  $Z=79$ ,  $T_1=0.500$  MeV.

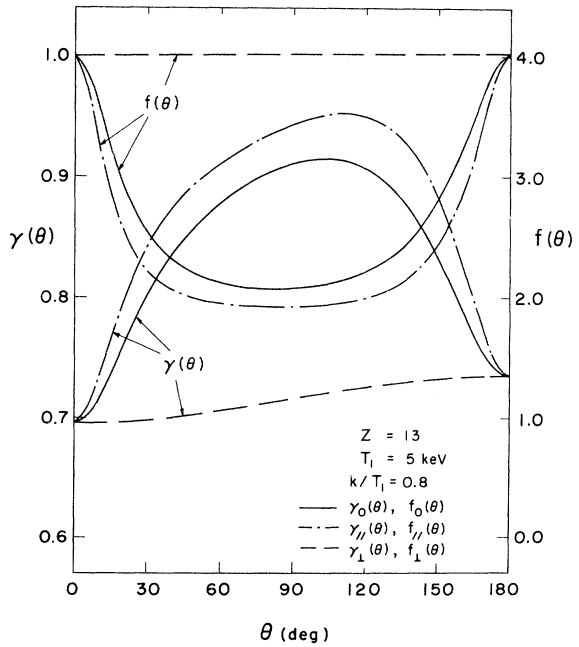


FIG. 11. Screening effects and Coulomb effects on the unpolarized cross sections and the polarized cross sections corresponding to that where the photon is either parallel or perpendicular to the emission plane for the case with  $Z=13$ ,  $T_1=5$  keV,  $k/T_1=0.8$ .

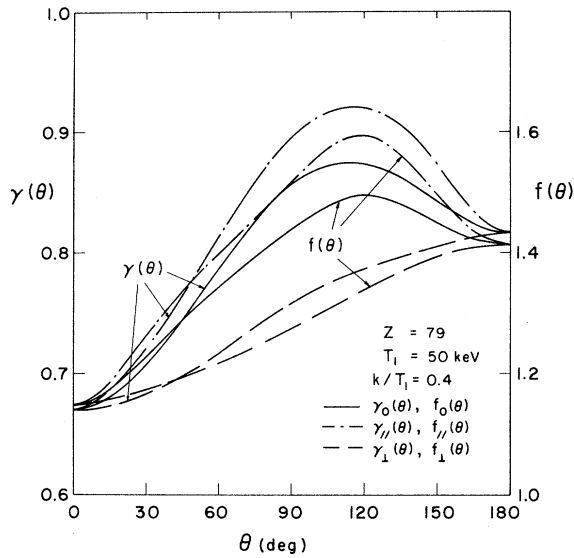


FIG. 12. Same as Fig. 11 except that  $Z=79$ ,  $T_1=50$  keV,  $k/T_1=0.4$ .

parallel (or perpendicular) to the emission plane. Nonrelativistically,<sup>9</sup> the correlation  $C_{03}$  is always positive. In the extreme high-energy limit<sup>10</sup> as

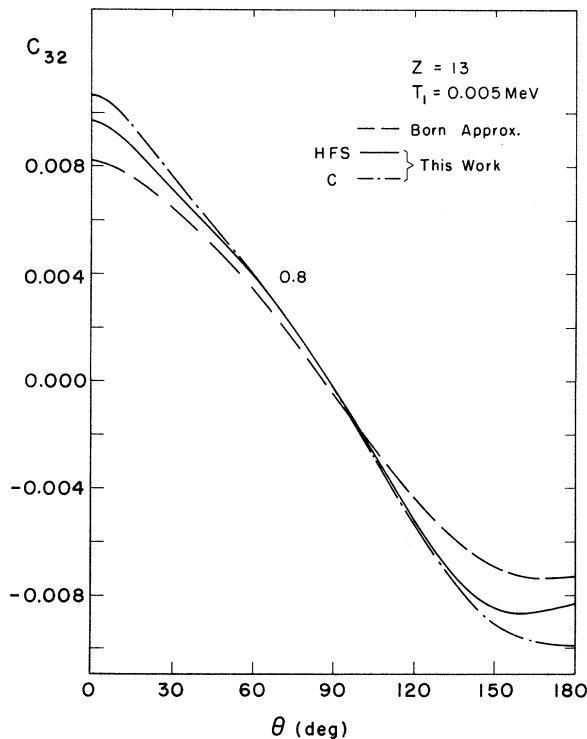


FIG. 13. Atomic bremsstrahlung-polarization correlation  $C_{32}$  for the case  $Z=13$ ,  $T_1=0.005$  MeV. The symbols C and HFS refer to the point-Coulomb potential and the Hartree-Fock-Slater potential with  $\frac{2}{3}$  of the Slater's exchange, respectively. The numbers attached to the curves give the value of  $k/T_1$  unless otherwise specified.

well as in the limit of Born approximation<sup>7</sup>  $C_{03}$  is of order 1—i. e., they do not vanish with large  $E$  or small  $Z$ . At high energies,<sup>10</sup>  $C_{03}$  is small at the tip of the spectrum and has its maximum value at the soft-photon limit.

Results of our numerical calculation of the polarization correlation  $C_{03}$  are given in Figs. 1–10. The correlation exhibits a “crossover” feature: For photon energies above some minimum energy radiation polarized in the emission plane is favored for smaller angles of emission (as predicted by the nonrelativistic theory), whereas polarization perpendicular to the plane is favored at larger angles. The maximum value of the correlation is approximately  $k/T_1$  for low  $Z$  and low energy. In the energy region considered in this paper, atomic-electron screening does affect the polarization correlation  $C_{03}$  in the same cases that it affected the unpolarized cross sections. Thus, if the correlation  $C_{03}$  is large and if the screening effect on the unpolarized cross section  $\sigma_0(k, \theta)$  is also large, i. e.,  $\gamma_0(\theta) \equiv \sigma_0^{\text{screened}}(k, \theta)/\sigma_0^{\text{Coulomb}}(k, \theta)$  differs considerably from 1, then the screening effect on the polarized cross sections  $\sigma_{||}(k, \theta)$  and  $\sigma_{\perp}(k, \theta)$  are quite different, where  $\sigma_{||}$  and  $\sigma_{\perp}$  are the cross sections corresponding to that the photon is polarized parallel or perpendicular to the emission plane. Sample results for  $\gamma_0(\theta)$ ,  $\gamma_{||}(\theta)$ , and  $\gamma_{\perp}(\theta)$  are given in Figs. 11 and 12. The corresponding integrated results

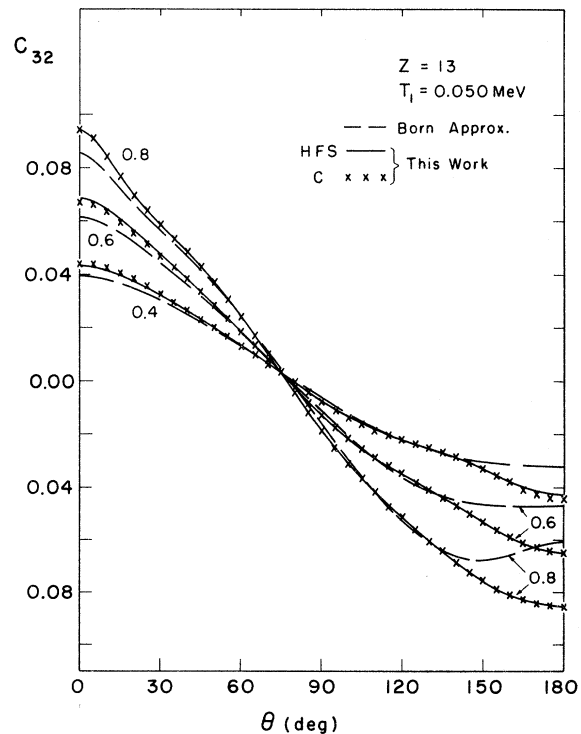


FIG. 14. Same as Fig. 13 except that  $Z=13$ ,  $T_1=0.050$  MeV.



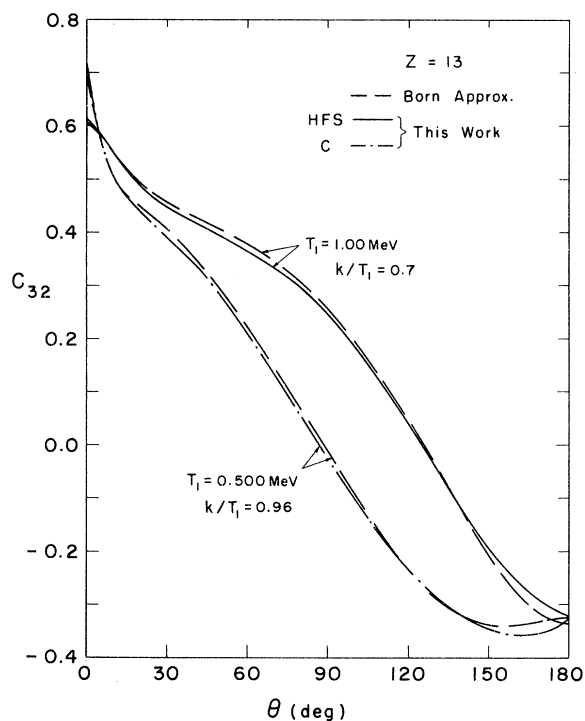


FIG. 15. Same as Fig. 13 except that  $Z=13$ ,  $T_1=0.500$  and 1.00 MeV.

are given in Tables I-III. In Figs. 11 and 12 and Tables I-III we show also the Coulomb effects (i. e., higher Born-approximation corrections)  $f_0(\theta)$ ,  $f_{II}(\theta)$ ,  $f_I(\theta)$ , and their integrated values, where we defined

$$f = \sigma^C / \sigma^B$$

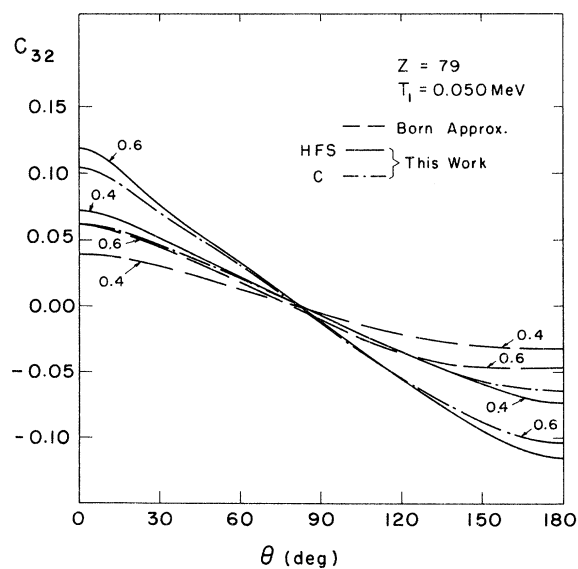


FIG. 16. Same as Fig. 13 except that  $Z=79$ ,  $T_1=0.050$  MeV.

TABLE I. Bremsstrahlung unpolarized and polarized cross sections  $\sigma(k) \equiv (k/Z^2)(d\sigma/dk)$ , showing electron screening and Coulomb effects for  $Z=13$ ,  $T_1=5$  keV,  $k/T_1=0.8$ . Symbols  $B$ ,  $C$ , and HFS refer to the Born approximation, and the point-Coulomb potential and the Hartree-Fock-Slater potential with two-thirds Slater's exchange, respectively ( $\gamma \equiv \sigma^s/\sigma^c$ ,  $f \equiv \sigma^c/\sigma^B$ ).

	$\sigma_B(k)$ (mb)	$\sigma_C(k)$ (mb)	$\sigma_{HFS}(k)$ (mb)	$\gamma$	$f$
$\sigma_0$	152.0	335.2	295.7	0.882	2.21
$\sigma_{II}$	136.4	272.4	250.9	0.921	2.00
$\sigma_L$	15.6	62.8	44.8	0.713	4.02
$\sigma_{TR}$	75.5	166.7	147.0	0.882	2.21
$\sigma_{TL}$	76.5	168.5	148.7	0.882	2.20
$\sigma_{LR}$	76.0	167.7	147.9	0.882	2.21
$\sigma_{LL}$	76.0	167.5	147.8	0.882	2.20

with the symbols  $B$  and  $C$  referring to the Born approximation and the point-Coulomb potential, respectively. Coulomb effects, like screening effects, show dependence on the polarization state.

The Born-approximation<sup>9</sup> results for the polarization correlation  $C_{03}$  are quite good for low- $Z$  cases whenever electron screening is not important, as shown in Figs. 1 and 3-5. We also present in Figs. 1, 3, 4, 6-8, and 10 comparisons with existing experiments. (In the energy region we consider here  $C_{03}$  is the only correlation for which experimental data exist.) Agreement with the experiments of Scheer, Trott, and Zahs<sup>5</sup> (STZ) is good. The older experimental data of Motz and Placious<sup>4</sup> (MP) deviate from our predictions as in their unpolarized cases. Our results generally agree better with the recent experimental data of Kuckuck and Ebert<sup>6</sup> (KE), as

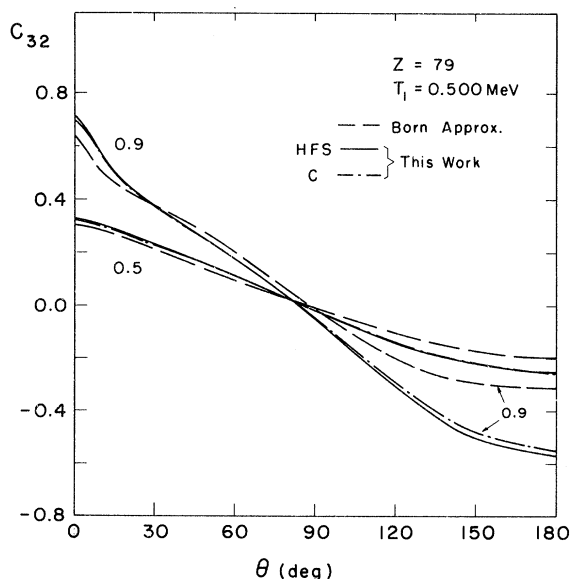


FIG. 17. Same as Fig. 13 except that  $Z=79$ ,  $T_1=0.500$  MeV.

TABLE II. Same as Table I except that  $Z=79$ ,  $T_1=50$  keV,  $k/T_1=0.4$ .

	$\sigma_B(k)$ (mb)	$\sigma_C(k)$ (mb)	$\sigma_{HFS}(k)$ (mb)	$\gamma$	$f$
$\sigma_0$	34.46	46.72	37.29	0.798	1.36
$\sigma_{11}$	22.58	31.95	26.47	0.828	1.41
$\sigma_{1L}$	11.88	14.77	10.82	0.733	1.24
$\sigma_{TR}$	16.74	23.34	18.69	0.801	1.39
$\sigma_{TL}$	17.72	23.38	18.60	0.796	1.32
$\sigma_{LR}$	17.36	23.58	18.80	0.797	1.36
$\sigma_{LL}$	17.10	23.14	18.49	0.799	1.35

shown in Figs. 6 and 7, though there are still discrepancies (see, e.g., Fig. 6).

#### D. Other Polarization Correlations

The polarization correlation  $C_{32}$ , shown in Figs. 13–17, is a transmitter of helicity, producing circularly polarized photons from longitudinally polarized electrons:

$$C_{32} = \frac{\sigma_{LR}(k, \theta) - \sigma_{LL}(k, \theta)}{\sigma_0(k, \theta)},$$

where  $\sigma_{LR}$  and  $\sigma_{LL}$  are the cross sections corresponding to the emission of circularly polarized

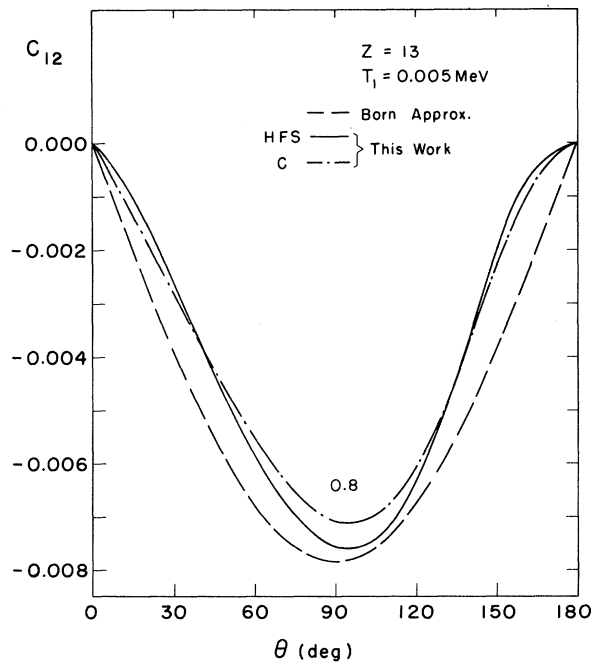


FIG. 18. Atomic bremsstrahlung-polarization correlation  $C_{12}$  for the case  $Z=13$ ,  $T_1=0.005$  MeV. The symbols C and HFS refer to the point-Coulomb potential and the Hartree-Fock-Slater potential with  $\frac{2}{3}$  of the Slater's exchange, respectively. The numbers attached to the curves give the value of  $k/T_1$  unless otherwise specified.

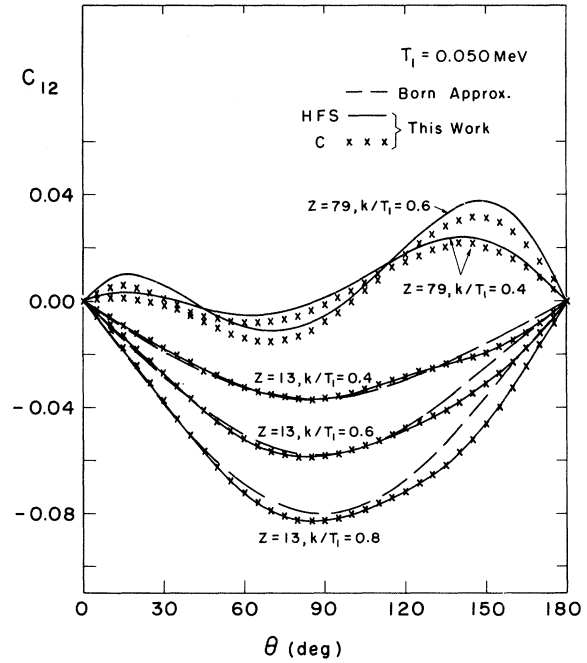


FIG. 19. Same as Fig. 18 except that  $Z=13, 79$  and  $T_1=0.050$  MeV.

positive- (negative) helicity photons from longitudinally polarized electrons. [Here we chose  $\hat{\epsilon}_R = z^{-1/2}(\epsilon_1 \hat{x} + i\epsilon_2 \hat{y})$  and  $\hat{\epsilon}_L = z^{-1/2}(\epsilon_1 \hat{x} - i\epsilon_2 \hat{y})$ .] This is the only polarization correlation which does not vanish in the forward and backward directions. However, like all correlations except  $C_{03}$ ,  $C_{32}$  vanishes in the nonrelativistic limit.<sup>9</sup> In the extreme-high-

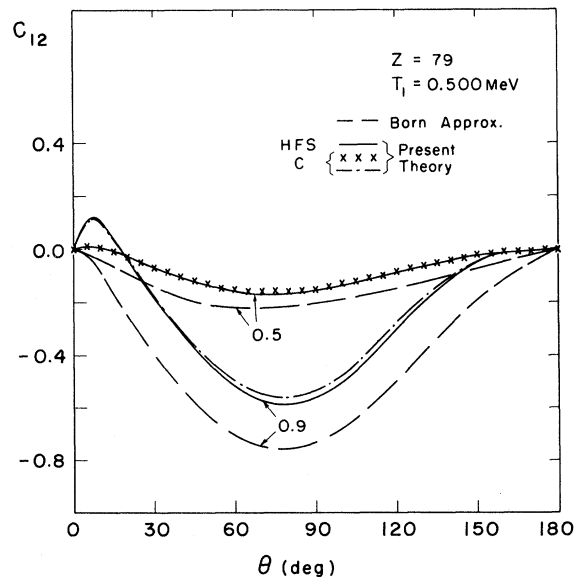


FIG. 20. Same as Fig. 18 except that  $Z=79$ ,  $T_1=0.500$  MeV.

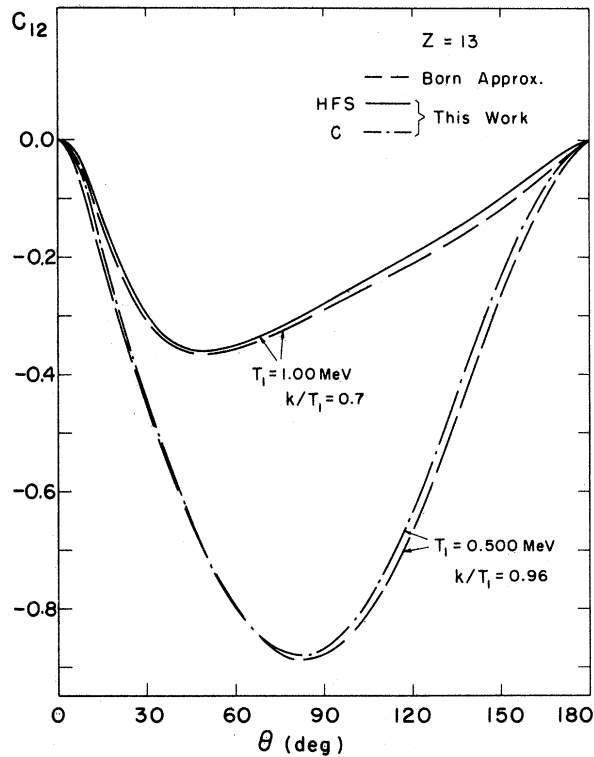


FIG. 21. Same as Fig. 18 except that  $Z=13$ ,  $T_1=0.500$  and  $1.00$  MeV.

energy limit<sup>10</sup> as well as in the limit of the Born approximation,<sup>7</sup> like  $C_{03}$  and  $C_{12}$ ,  $C_{32}$  is of order 1. In the extreme-high-energy limit the circular polar-

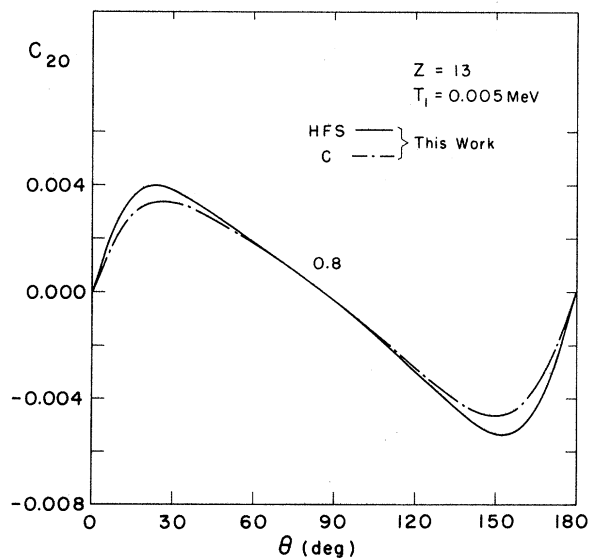


FIG. 22. Atomic bremsstrahlung-polarization correlation  $C_{20}$  for the case  $Z=13$ ,  $T_1=0.005$  MeV. The symbols  $C$  and HFS refer to the point-Coulomb potential and the Hartree-Fock-Slater potential with  $\frac{2}{3}$  of the Slater's exchange, respectively. The numbers attached to the curves give the value of  $k/T_1$  unless otherwise specified.

TABLE III. Same as Table I except that  $Z=79$ ,  $T_1=500$  keV,  $k/T_1=0.9$ .

	$\sigma_B(k)$ (mb)	$\sigma_C(k)$ (mb)	$\sigma_{\text{HFS}}(k)$ (mb)	$\gamma$	$f$
$\sigma_0$	1.368	5.143	4.856	0.944	3.76
$\sigma_{11}$	1.060	3.816	3.637	0.953	3.60
$\sigma_L$	0.308	1.327	1.219	0.919	4.31
$\sigma_{TR}$	0.410	2.006	1.859	0.927	4.89
$\sigma_{TL}$	0.958	3.137	2.997	0.955	3.27
$\sigma_{LR}$	0.926	3.405	3.211	0.943	3.68
$\sigma_{LL}$	0.442	1.738	1.645	0.946	3.93

ization from longitudinally polarized electrons has the opposite energy dependence from the linear polarization. It is large for relatively hard quanta while small for relatively soft quanta. At the tip of the photon spectrum this circular-polarization transfer is complete. For not too low energies and low- $Z$  elements the Born-approximation results are quite good. The atomic-electron screening effect on the polarization correlation  $C_{32}$  is small. Sample results for  $\gamma_{LR}$  and  $\gamma_{LL}$  are given in Tables I-III.

The polarization correlation  $C_{12}$ , shown in Figs. 18-21, produces circularly polarized photons from electrons transversely polarized in the emission plane, namely,

$$C_{12} = \frac{\sigma_{TR}(k, \theta) - \sigma_{TL}(k, \theta)}{\sigma_0(k, \theta)},$$

where  $\sigma_{TR}$  and  $\sigma_{TL}$  are the polarized cross sections

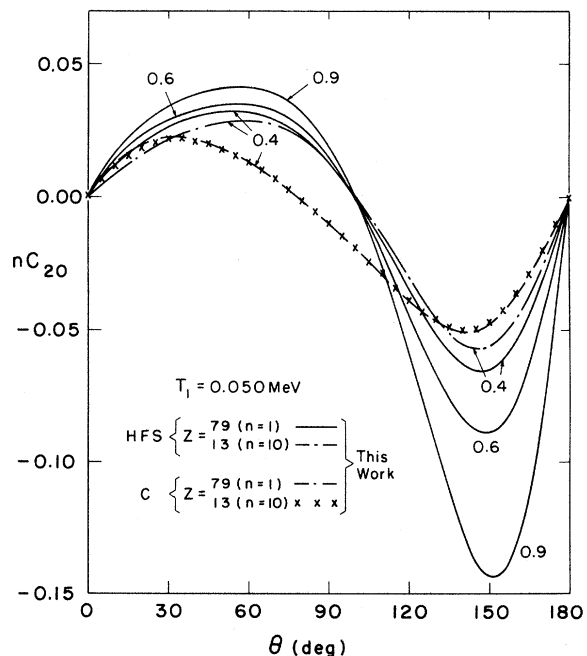


FIG. 23. Same as Fig. 22 except that  $Z=13, 79$  and  $T_1=0.050$  MeV.

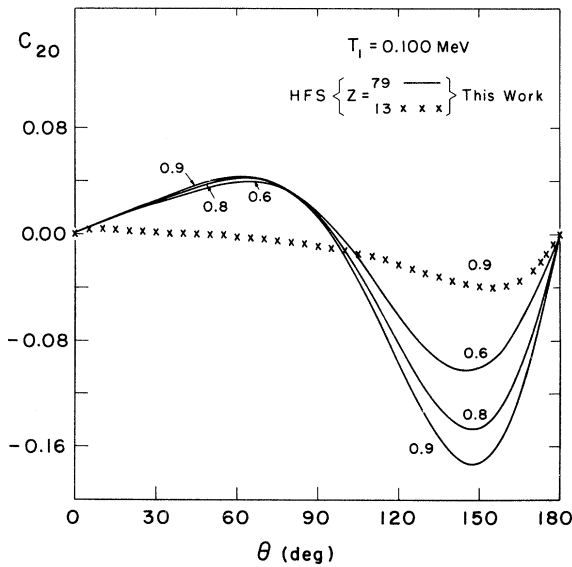


FIG. 24. Same as Fig. 22 except that  $Z=13, 79$  and  $T_1=0.100$  MeV.

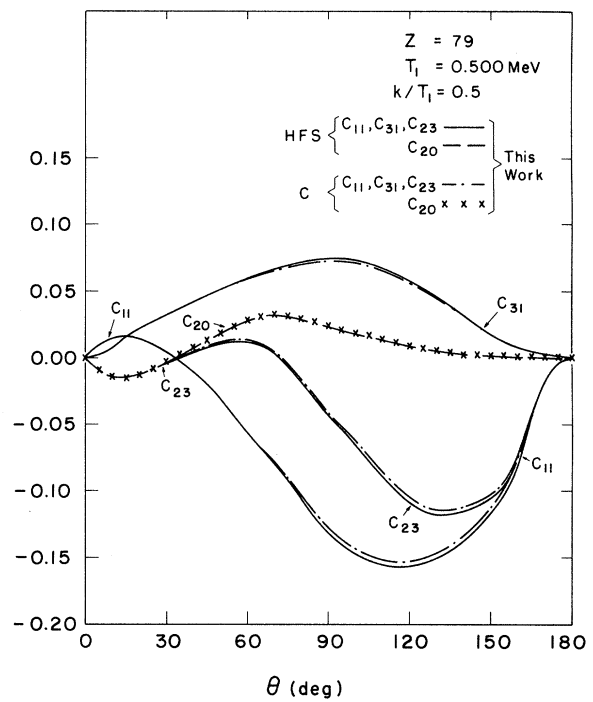


FIG. 26. The atomic bremsstrahlung-polarization correlations  $C_{20}, C_{11}, C_{31}$ , and  $C_{23}$  for the case  $Z=79, T_1=0.500$  MeV,  $k/T_1=0.5$ .

corresponding to the emission of circularly polarized positive- (negative) helicity photons from transversely polarized electrons. The correlation vanishes in the nonrelativistic theory.<sup>9</sup> In the extreme-

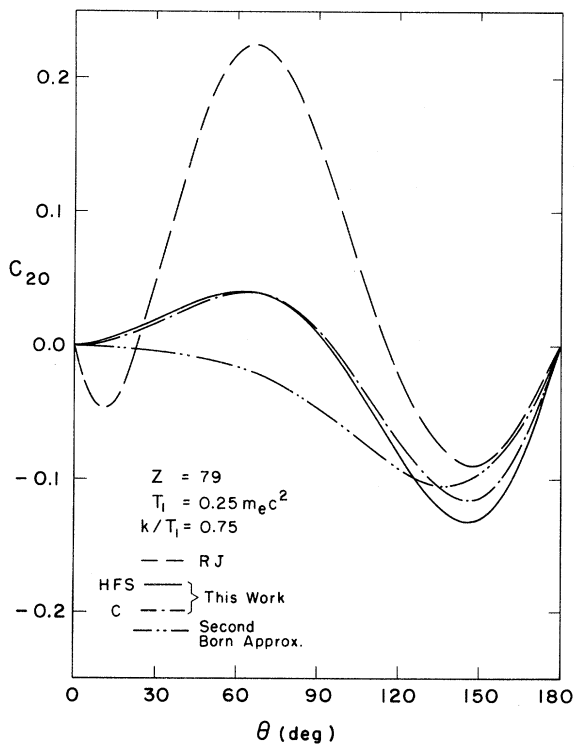


FIG. 25. Same as Fig. 22 except that  $Z=79, T_1=0.25m_e c^2$ ,  $k/T_1=0.75$ .

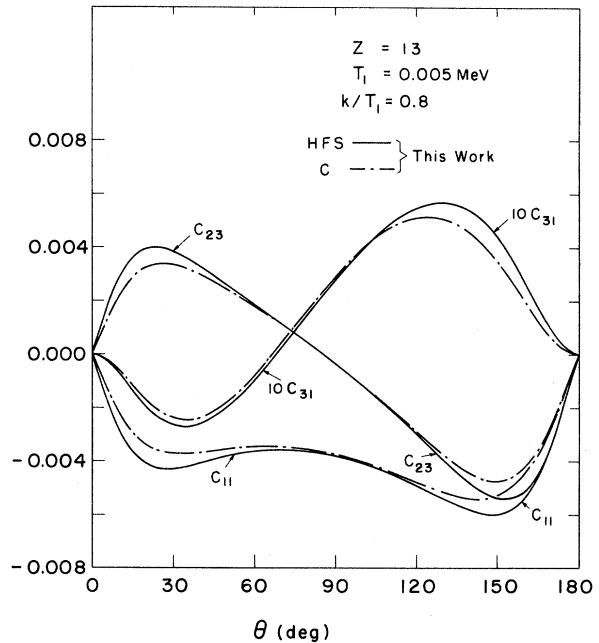


FIG. 27. The atomic bremsstrahlung-polarization correlations  $C_{11}, C_{31}$ , and  $C_{23}$  for the case  $Z=13, T_1=0.005$  MeV,  $k/T_1=0.8$ . The symbols C and HFS refer to the point-Coulomb potential and the Hartree-Fock-Slater potential with  $\frac{2}{3}$  of the Slater's exchange, respectively.

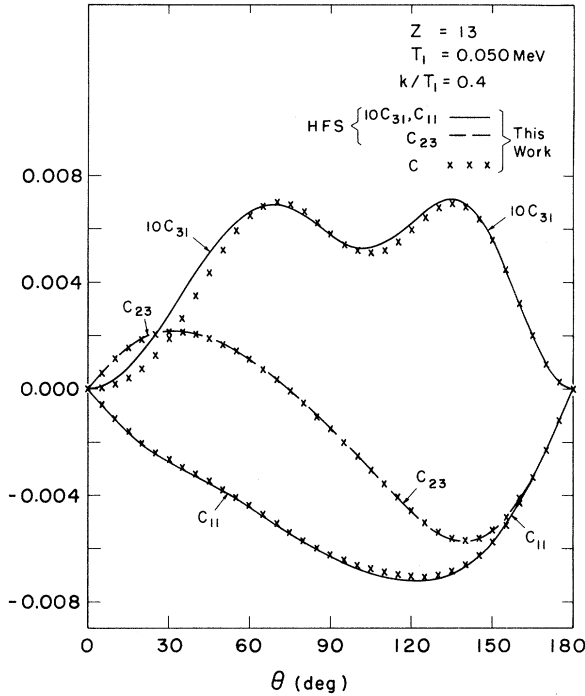


FIG. 28. Same as Fig. 27 except that  $Z=13$ ,  $T_1=0.050$  MeV,  $k/T_1=0.4$ .

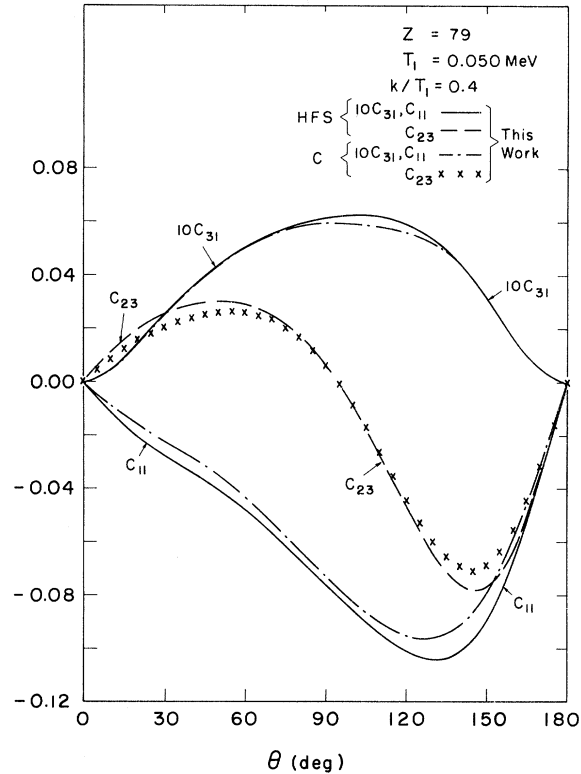


FIG. 29. Same as Fig. 27 except that  $Z=79$ ,  $T_1=0.050$  MeV,  $k/T_1=0.4$ .

high-energy limit<sup>10</sup> as well as in the limit of the Born approximation,<sup>7</sup> like  $C_{03}$  and  $C_{32}$ ,  $C_{12}$  is of order 1. Born-approximation results are quite good for low- $Z$  elements but for high- $Z$  elements the difference between the Born results and ours is very large. The atomic-electron screening effect on  $C_{12}$  is again small. Sample results for  $\gamma_{TR} = \sigma_{TR}^s / \sigma_{TR}^c$  and  $\gamma_{TL} = \sigma_{TL}^s / \sigma_{TL}^c$  are given in Tables I-III.

The polarization correlation  $C_{20}$ , shown in Figs. 22-26, is an analyzer for transversely polarized electrons in the case that the initial electron spin is perpendicular to the emission plane. The polarization correlation  $C_{20}$  vanishes both in the nonrelativistic<sup>9</sup> and extreme relativistic<sup>10</sup> limits and is<sup>7,18</sup> of order of  $a = Z\alpha$ . In Fig. 25 we show comparisons of our results with those of Rozics and Johnson<sup>11</sup> (RJ) and of the second Born approximation<sup>18</sup> for  $Z=79$ . We disagree with these results.

The polarization correlation  $C_{23}$ , shown in Figs. 26-29, involves the production of linearly polarized photons from transversely polarized electrons. To determine  $C_{23}$  will require also determining  $C_{20}$  and  $C_{03}$ , or at least designing a set of experiments which subtract out their effects;  $C_{23}$  is the only one of the seven polarization correlations which cannot

be determined independently. Like  $C_{20}$ , the polarization correlation  $C_{23}$  vanishes in the nonrelativistic and the extreme-high energy<sup>10</sup> limits and is of order of  $a$ . For small photon angles we have  $C_{23} = C_{11}$ , while for large angles we have  $C_{23} = +C_{11}$ .

The polarization correlation  $C_{11}$ , shown in Figs. 26-29, like  $C_{23}$ , produces linearly polarized photons from transversely polarized electrons. However, this correlation, also of order  $a$ , is between electrons polarized in the emission plane and photons polarized at  $45^\circ$  to the emission plane. It vanishes in the nonrelativistic<sup>9</sup> and the extreme-high-energy<sup>10</sup> limits. For very small photon angles we have  $C_{11} = -C_{23}$ , while for large angles we have  $C_{11} = +C_{23}$ .

The polarization correlation  $C_{31}$ , shown in Figs. 26-29, which is of order  $a$ , produces linearly polarized photons from longitudinally polarized electrons. The photon polarization is again at  $45^\circ$  to the emission plane. This correlation also vanishes in the nonrelativistic<sup>9</sup> limit and the extreme-high-energy<sup>10</sup> limit.

\*Supported in part by the National Science Foundation under Grant No. GP-32798.

<sup>1</sup>H. K. Tseng and R. H. Pratt, Phys. Rev. A **3**, 100 (1971). We follow the same notations used in this paper and use again the

unrationalized units, i.e.,  $\hbar = m_e = c = 1$  throughout, unless specified.

<sup>2</sup>H. Aiginger, Z. Phys. **197**, 8 (1966), and private communication; D. H. Rester and W. E. Dance, Phys. Rev.

- 161, 85 (1967); D. H. Rester, N. Edmonson, and Q. Peasley, *Phys. Rev. A* **2**, 2190 (1970).
- <sup>3</sup>H. Frauenfelder, R. Bobone, E. von Goeler, N. Levine, H. R. Lewis, R. N. Peacock, A. Rossi, and G. DePasquali, *Phys. Rev.* **106**, 386 (1957); G. Culligan, S. G. F. Frank, J. R. Holt, J. C. Kluyver, and T. Massam, *Nature (Lond.)* **180**, 751 (1957).
- <sup>4</sup>J. W. Motz and R. C. Placious, *Nuovo Cimento* **15**, 571 (1960).
- <sup>5</sup>M. Scheer, E. Trott, and G. Zahr, *Z. Phys.* **209**, 68 (1968).
- <sup>6</sup>R. W. Kuckuck, Ph.D. thesis (University of California, 1972), Lawrence Livermore Laboratory, Report No. UCRL-51188 (unpublished); R. W. Kuckuck and P. J. Ebert, *Phys. Rev. A* **7**, 456 (1973).
- <sup>7</sup>R. L. Gluckstern, M. H. Hull, Jr., and G. Breit, *Phys. Rev.* **90**, 1026 (1953); R. L. Gluckstern and M. H. Hull, Jr., *Phys. Rev.* **90**, 1030 (1953); H. Banerjee, *Phys. Rev.* **111**, 532 (1968); K. W. McVoy, *Phys. Rev.* **106**, 826 (1957); *Phys. Rev.* **111**, 1333 (1958); C. Fronsdal and H. Überall, *Phys. Rev.* **111**, 580 (1958).
- <sup>8</sup>H. A. Bethe and W. Heitler, *Proc. R. Lond. A* **146**, 83 (1934).
- <sup>9</sup>P. Kirkpatrick and L. Wiedmann, *Phys. Rev.* **67**, 321 (1945).
- <sup>10</sup>H. Olsen and L. C. Maximon, *Phys. Rev.* **110**, 589 (1958); *Phys. Rev.* **114**, 887 (1959).
- <sup>11</sup>J. D. Rozics and W. R. Johnson, *Phys. Rev.* **135**, B56 (1964).
- <sup>12</sup>H. Brysk, C. D. Zerby, and S. K. Penny, *Phys. Rev.* **180**, 104 (1969).
- <sup>13</sup>E. Haug, *Phys. Rev.* **188**, 63 (1969).
- <sup>14</sup>Hsiang-Kuang Tseng, Ph.D. thesis (University of Pittsburgh, 1970) (unpublished).
- <sup>15</sup>See, for example, V. B. Berestetskii, E. M. Lifshitz, and L. P. Pitaevskii, *Relativistic Quantum Theory*, translated by J. B. Sykes and J. S. Bell (Pergamon, New York, 1971), Part 1; H. A. Tolhoek, *Rev. Mod. Phys.* **28**, 277 (1956); W. H. McMaster, *Rev. Mod. Phys.* **33**, 8 (1961).
- <sup>16</sup>Here we follow the argument of B. Nagel [*Ark. Fys.* **18**, 1 (1960)].
- <sup>16a</sup>See, for example, J. D. Bjorken and S. D. Drell, *Relativistic Quantum Mechanics* (McGraw-Hill, New York, 1964), pp. 72 and 73.
- <sup>17</sup>For atomic photoelectric effect see, for example, B. Nagel, *Ark. Fys.* **18**, 1 (1960); R. H. Pratt, R. D. Levee, R. L. Pexton, and W. Aron, *Phys. Rev.* **134**, A916 (1964).
- <sup>18</sup>W. R. Johnson and J. D. Rozics, *Phys. Rev.* **128**, 192 (1962); E. S. Sobolak and P. Stehle, *Phys. Rev.* **129**, 403 (1963).

## Proposed Method for Computing Dynamic Polarizabilities of Atoms\*

William A. Sanders

*Center for Molecular Dynamics and Energy Transfer, Department of Chemistry, The Catholic University of America, Washington, D. C. 20017*

(Received 6 December 1972)

It has been shown recently that static polarizabilities can be computed efficiently by solving the multiconfigurational self-consistent-field equations for an atom in the presence of a point charge which provides the polarizing field. The formalism developed here is designed to take advantage of these calculations in the computation of dynamic polarizabilities. The approach is basically equivalent to a perturbation method in which the unperturbed state is the statically polarized atom. The transition to the time-dependent problem is effected by introducing a potential function which turns off the static field and turns on a dynamic field with the desired time dependence. The spatial parts of the time-dependent wave function are represented by linear combinations of the statically polarized configurations, without explicit reference to the orbital model.

### I. INTRODUCTION

In calculating the response of an atom to an external field, the usual approach is to make use of a version of the coupled perturbed Hartree-Fock (CPHF) method.<sup>1-6</sup> This model starts with the unperturbed Hartree-Fock (HF) wave function of the atom and leads to a set of coupled integrodifferential equations for the first-order corrections to the atomic orbitals. These equations are generally solved by expanding the first-order orbitals in an appropriate set of basis functions, thereby transforming to a set of matrix equations.

A critical step in the application of the CPHF method to the calculation of atomic polarizabilities is the selection of an efficient basis set. Since the external field couples the unperturbed HF orbitals to orbitals of different parity, the HF basis must be augmented with suitably chosen polarization functions. It is imperative that this set of func-

tions be compact if the magnitude of the computation is to be kept within reasonable bounds.

Alexander and Gordon<sup>6</sup> circumvented the problem of choosing the basis functions by solving the first-order CPHF equations exactly for the He atom. Their method worked quite efficiently and provided a convenient set of exact values against which other calculations can be measured.

Recently, Billingsley and Krauss<sup>7</sup> demonstrated a practical method for calculating the response of an atom to a static multipole field. Their approach is to solve the multiconfigurational self-consistent-field<sup>8</sup> (MCSCF) equations directly for the atom in the presence of a charged particle which simulates the external perturbing field. The coupling to functions of different parity which results from the relaxation of the spherical symmetry of the atom in the presence of the field is optimized directly through the variation principle. Furthermore, a prescription was developed for choosing a suffi-